# Influence of streamwise vortices on Tollmien–Schlichting waves

Ali H. Nayfeh and Ayman Al-Maaitah
*Engineering Science and Mechanics Department, Virginia Polytechnic Institute and State University, Blacksburg, Virginia 24061*

(Received 15 December 1987; accepted 7 September 1988)

An analysis is presented of the influence of steady quasiperiodic streamwise vortices on Tollmien–Schlichting (TS) waves. The vortices act as parametric exciters for the TS waves. The present analysis is for the subharmonic resonance in which the spanwise wavenumber of the vortices is twice that of the TS wave. Floquet theory is used to derive an eigenvalue problem for the complex streamwise wavenumber, which is then solved using a shooting technique. The results show that there are two components of the solution, one is stabilized and the other is destabilized by the vortices. For the same flow characteristics, calculations were obtained from the theory which Nayfeh [J. Fluid Mech. **107**, 441 (1981)] developed using the method of multiple scales. The results obtained from both approaches are in excellent agreement.

## I. INTRODUCTION

The purpose of the present paper is to study the influence of steady streamwise vortices, especially Goertler vortices, on oblique Tollmien–Schlichting (TS) waves.

Using the method of multiple scales, Nayfeh[1] showed that streamwise vortices act as parametric exciters for selected oblique Tollmien–Schlichting waves, and to first order, the selected waves have a spanwise wavelength that is twice that of the vortices. Nayfeh derived an expression for the additional growth caused by the vortices. It has the form of a double exponential. Similar double exponentials were also suggested by Herbert and Morkovin[2] for the influence of TS waves on streamwise vortices and by Floryan and Saric[3] for the influence of Goertler vortices on streamwise vortices. Using a Fourier–Chebyshev spectral method, Malik[4] obtained results that do not agree with the numerical results obtained previously by Nayfeh. Srivastava and Dallman[5] conducted an analysis similar to Nayfeh's analysis and reproduced his evolution equations for the amplitudes of the Tollmien–Schlicting waves with streamwise position. Moreover, they performed numerical calculations for the same parameters Nayfeh used and obtained results for the first-order problem, Goertler vortices, and the influence of the vortices on Tollmien–Schlichting waves that fully agree with Nayfeh's results. Upon a closer examination of the numerical results of Nayfeh, we found that the characteristic length scale used to calculate the Goertler vortices is different from that used to calculate the Tollmien–Schlichting waves. Therefore we reconsider the problem and reformulate it using Floquet theory. Both theories indicate that Goertler vortices result in the amplitude of TS waves having two components—one grows slower and the other grows faster than the unexcited TS waves.

Bennett and Hall[6] used triple-deck theory to analyze the influence of Taylor–Goertler vortices in fully developed flows on TS waves. They found that although the maximum growth rate as a function of frequency is not greatly affected, there is a large destabilizing effect over a large range of frequencies.

## II. PROBLEM FORMULATION

We consider the linear three-dimensional stability of a basic flow consisting of the sum of a two-dimensional boundary-layer flow $[U_0(x_1, y),\ \epsilon V_0(x_1, y)$, and $P_0(x_1)]$ and a growing steady quasiperiodic counter-rotating vortex flow:

$$\hat{u} = \epsilon_v U_1(x_1, z_1, y)\cos 2\beta z, \tag{1}$$

$$\hat{v} = \epsilon_v V_1(x_1, z_1, y)\cos 2\beta z, \tag{2}$$

$$\hat{w} = \epsilon_v W_1(x_1, z_1, y)\sin 2\beta z, \tag{3}$$

$$\hat{p} = \epsilon_v P_1(x_1, z_1, y)\cos 2\beta z, \tag{4}$$

where $x_1 = \epsilon x$, $z_1 = \epsilon_1 z$, and $\epsilon$ and $\epsilon_1$ are small dimensionless parameters that characterize the growth of the boundary layer and quasiperiodicity of the vortices. The strength of the vortices is $\epsilon_v$ and their growth rate is given by

$$\sigma_G = \frac{d\epsilon_v}{dx}. \tag{5}$$

Thus the basic flow whose stability is to be investigated has the form

$$U = U_0(x_1, y) + \epsilon_v U_1(x_1, z_1, y)\cos 2\beta z, \tag{6}$$

$$V = \epsilon V_0(x_1, y) + \epsilon_v V_1(x_1, z_1, y)\cos 2\beta z, \tag{7}$$

$$W = \epsilon_v W_1(x_1, z_1, y)\sin 2\beta z, \tag{8}$$

$$P = P_0(x_1) + \epsilon_v P_1(x_1, z_1, y)\cos 2\beta z. \tag{9}$$

In Eqs. (6)–(9), velocities are made dimensionless using a reference velocity $U_r$ and a reference boundary-layer length scale $\delta_r$. We superimpose the small unsteady perturbation quantities $\epsilon_T u(x, y, z, t)$, $\epsilon_T v(x, y, z, t)$, $\epsilon_T w(x, y, z, t)$, and $\epsilon_T p(x, y, z, t)$ on those given in Eqs. (6)–(9), so that the total flow quantities become $U + \epsilon_T u$, $V + \epsilon_T v$, $W + \epsilon_T w$, and $P + \epsilon_T p$. Here, $\epsilon_T$ is a small dimensionless quantity that is of the order of the amplitude of the Tollmien–Schlichting waves. In this paper, we assume that $\epsilon_T$ is small compared with $\epsilon_v$, so that the streamwise vortices influence, but are not influenced by, the Tollmien–Schlichting waves. Substituting the total-flow quantities into the Navier–Stokes equations, subtracting the basic-flow quantities, and linearizing the resulting equations, we obtain

 0031-9171/88/123543-07$01.90  

$$\frac{\partial u}{\partial x}+\frac{\partial v}{\partial y}+\frac{\partial w}{\partial z}=0, \tag{10}$$

$$\begin{aligned}\frac{\partial u}{\partial t}&+U_0\frac{\partial u}{\partial x}+v\frac{\partial U_0}{\partial y}+\frac{\partial p}{\partial x}-\frac{1}{R}\nabla^2 u\\&=-\epsilon_v\Big[\Big(U_1\frac{\partial u}{\partial x}+V_1\frac{\partial u}{\partial y}+\frac{\partial U_1}{\partial y}v+\sigma_G U_1 u\Big)\\&\quad\times\cos 2\beta z+\Big(W_1\frac{\partial u}{\partial z}-2\beta U_1 w\Big)\sin 2\beta z\Big]\\&\quad-\epsilon\Big(\frac{\partial U_0}{\partial x_1}u+V_0\frac{\partial u}{\partial y}\Big)+\cdots,\end{aligned} \tag{11}$$

$$\begin{aligned}\frac{\partial v}{\partial t}&+U_0\frac{\partial v}{\partial x}+\frac{\partial p}{\partial y}-\frac{1}{R}\nabla^2 v\\&=-\epsilon_v\Big[\Big(U_1\frac{\partial v}{\partial x}+V_1\frac{\partial v}{\partial y}+\frac{\partial V_1}{\partial y}v+\sigma_G V_1 u\Big)\\&\quad\times\cos 2\beta z+\Big(W_1\frac{\partial v}{\partial z}-2\beta V_1 w\Big)\sin 2\beta z\Big]\\&\quad-\epsilon\Big(V_0\frac{\partial v}{\partial y}+\frac{\partial V_0}{\partial y}v\Big)+\cdots,\end{aligned} \tag{12}$$

$$\begin{aligned}\frac{\partial w}{\partial t}&+U_0\frac{\partial w}{\partial x}+\frac{\partial p}{\partial z}-\frac{1}{R}\nabla^2 w\\&=-\epsilon_v\Big[\Big(U_1\frac{\partial w}{\partial x}+V_1\frac{\partial w}{\partial y}+2\beta W_1 w\Big)\cos 2\beta z\\&\quad+\Big(\frac{\partial W_1}{\partial y}v+W_1\frac{\partial w}{\partial z}+\sigma_G W_1 u\Big)\sin 2\beta z\Big]\\&\quad-\epsilon V_0\frac{\partial w}{\partial y}+\cdots,\end{aligned} \tag{13}$$

where $R=U_r\delta_r/\nu$ and $\nu$ is the kinematic viscosity of the fluid. The boundary conditions are

$$u=v=w=0,\quad \text{at } y=0, \tag{14}$$

$$u,v,w,\to 0,\quad \text{as } y\to\infty. \tag{15}$$

For parallel flows $U_0$ is a weak function of $x$ and $V_0 \ll U_0$. Letting $\epsilon\to 0$ the terms multiplied by $\epsilon$ will then drop out from Eqs. (10)–(13) and $U_0$, $V_0$, $U_1$, $V_1$, and $W_1$ will be functions of $y$ only. This is the quasiparallel assumption.

In this paper, we determine the influence of the vortices, including their growth rate $\sigma_G$, on the growth of the TS waves in a quasiparallel flow using Floquet theory.

## III. FLOQUET THEORY

Using the quasiparallel flow assumption, we find that the coefficients in Eqs. (10)–(13) are independent of $x$ and $t$, and when $\epsilon_v \neq 0$ these coefficients are periodic in $z$. Consequently, we can separate the $x$ and $t$ variation using the normal mode concept and use Floquet theory to express the disturbance in the form

$$(u,v,w,p)=[\hat u(y,z),\hat v(y,z),\hat w(y,z),\hat p(y,z)]\times\exp(i\theta+\gamma z), \tag{16}$$

$$\theta=\int \alpha\,dx-\omega t,$$

where $\gamma$, $\alpha$, and $\omega$ are complex in general, and $\hat u$, $\hat v$, $\hat w$, and $\hat p$ are periodic in $z$. Expanding $\hat u$, $\hat v$, $\hat w$, and $\hat p$ in a Fourier series, we express the disturbance as

$$u=e^{i\theta+\gamma z}\sum_{m=0}^{\infty}\xi_{1m}(y)(a_{1m}\cos m\beta z+b_{1m}\sin m\beta z), \tag{17a}$$

$$v=e^{i\theta+\gamma z}\sum_{m=0}^{\infty}\xi_{3m}(y)(a_{3m}\cos m\beta z+b_{3m}\sin m\beta z), \tag{17b}$$

$$p=e^{i\theta+\gamma z}\sum_{m=0}^{\infty}\xi_{4m}(y)(a_{4m}\cos m\beta z+b_{4m}\sin m\beta z), \tag{17c}$$

$$w=e^{i\theta+\gamma z}\sum_{m=0}^{\infty}\xi_{5m}(y)(a_{5m}\cos m\beta z+b_{5m}\sin m\beta z), \tag{17d}$$

where the $a_{nm}$ and $b_{nm}$ are constants.

Substituting Eqs. (17) into Eqs. (10)–(15) and equating the coefficients of the different harmonics of $z$, we obtain two separate sets of equations for even and odd $m$; that is, the disturbance decouples into the components

$$q_n^s=e^{i\theta+\gamma z}\sum_{m=\text{odd}}\xi_{nm}(a_{nm}\cos m\beta z+b_{nm}\sin m\beta z), \tag{18}$$

$$q_n^f=e^{i\theta+\gamma z}\sum_{m=\text{even}}\xi_{nm}(a_{nm}\cos m\beta z+b_{nm}\sin m\beta z), \tag{19}$$

where $q_n$ stands for $(u,v,p,w)$, $n=1$, 3, 4, and 5, $q_n^s$ denotes the subharmonic mode, and $q_n^f$ denotes the fundamental mode.

For our problem, $\beta$ is real and we consider the case in which the subharmonic and the fundamental modes are tuned. Hence we put $\gamma=0$. The lowest truncation of the series for the subharmonic mode corresponds to $m=1$, thereby including only $\xi_{n1}(a_{n1}\cos\beta+b_{n1}\sin\beta)$. On the other hand, the lowest truncation of the series for the fundamental mode contains $m=0$, 2, and 4. Our analysis is restricted to the subharmonic case. Upon the examination of Eqs. (17) and (10)–(13), we find that the solution in Eqs. (17) can split into two components. The first one is formed as follows:

$$u=\xi_1(y)\cos\beta z\exp i\Big(\int\alpha\,dx-\omega t\Big), \tag{20}$$

$$v=\xi_3(y)\cos\beta z\exp i\Big(\int\alpha\,dx-\omega t\Big), \tag{21}$$

$$p=\xi_4(y)\cos\beta z\exp i\Big(\int\alpha\,dx-\omega t\Big), \tag{22}$$

$$w=\xi_5(y)\sin\beta z\exp i\Big(\int\alpha\,dx-\omega t\Big), \tag{23}$$

where $\xi_n=\xi_{n1}a_{n1}$ for $n=1$, 3, and 4 and $\xi_5=\xi_{51}b_{51}$. The second component of the solution is 90° shifted in $z$ from the first one; namely,

$$u=\xi_1(y)\sin\beta z\exp i\Big(\int\alpha\,dx-\omega t\Big), \tag{24}$$

$$v=\xi_3(y)\sin\beta z\exp i\Big(\int\alpha\,dx-\omega t\Big), \tag{25}$$

$$p=\xi_4(y)\sin\beta z\exp i\Big(\int\alpha\,dx-\omega t\Big), \tag{26}$$

$$w=\xi_5(y)\cos\beta z\exp i\left(\int\alpha\,dx-\omega t\right), \qquad (27)$$

where $\xi_n=\xi_{n1}b_{n1}$ for $n=1$, 3, and 4 and $\xi_5=\xi_{51}a_{51}$.

This splitting of the solution into two components corresponds to the two growth rates that Nayfeh[1] found using the method of multiple scales. Substituting either Eqs. (20)–(23) or Eqs. (24)–(27) into Eqs. (10)–(13) and equating the coefficients of $\cos\beta z$ and $\sin\beta z$ on both sides yields the two eigenvalue problems

$$i\alpha\xi_1+D\xi_3+\beta\xi_5=0, \qquad (28)$$

$$\begin{aligned}&i(\alpha U_0-\omega)\xi_1+\xi_3\,DU_0+i\alpha\xi_4\\&\quad-(1/R)(D^2-\alpha^2-\beta^2)\xi_1\\&\quad=\pm\tfrac{1}{2}\epsilon_v(i\alpha U_1\xi_1+V_1\,D\xi_1+\xi_3\,DU_1\\&\qquad+\sigma_G U_1\xi_1-\beta W_1\xi_1-2\beta U_1\xi_5),\end{aligned} \qquad (29)$$

$$\begin{aligned}&i(\alpha U_0-\omega)\xi_3+D\xi_4-(1/R)(D^2-\alpha^2-\beta^2)\xi_3\\&\quad=\pm\tfrac{1}{2}\epsilon_v(i\alpha U_1\xi_3+V_1\,D\xi_3+\xi_3\,DV_1\\&\qquad+\sigma_G V_1\xi_1-\beta W_1\xi_3-2\beta V_1\xi_5),\end{aligned} \qquad (30)$$

$$\begin{aligned}&i(\alpha U_0-\omega)\xi_5-\beta\xi_4-(1/R)(D^2-\alpha^2-\beta^2)\xi_5\\&\quad=\pm\tfrac{1}{2}\epsilon_v(-i\alpha U_1\xi_5-V_1\,D\xi_5\\&\qquad-\beta W_1\xi_5+\xi_3\,DW_1+\sigma_G W_1\xi_1),\end{aligned} \qquad (31)$$

$$\xi_1=\xi_3=\xi_5=0,\quad\text{at } y=0, \qquad (32)$$

$$\xi_n\to 0,\quad\text{as } y\to\infty, \qquad (33)$$

where $D$ stands for $d/dy$, the negative sign corresponds to Eqs. (20)–(23), while the positive sign corresponds to Eqs. (24)–(27), which means that the two components of the solution correspond to two different vortices that are equal in magnitude, but opposite in direction.

In this paper, we consider the case of spatial stability in which $\omega$ is real and $\alpha=\alpha_r+i\alpha_i$ is complex with $-\alpha_i$ representing the growth rate. For a fixed physical dimensional frequency, $\omega$ is real and fixed by the dimensionless frequency $F=\omega/R$.

For a given spanwise wavenumber $\beta$, Goertler number GN, and Reynolds number $R$, we solved for the Goertler vortex to determine $U_1$, $V_1$, $W_1$, and $P_1$ and the corresponding $\sigma_G$. For a given frequency and $\epsilon_v$ and using the Goertler flow, we numerically solved the eigenvalue problem consisting of Eqs. (28)–(33) for the eigenvalue $\alpha$.

## IV. NUMERICAL PROCEDURE

To solve the eigenvalue problem in Eqs. (28)–(33) we need to find the mean flow velocity $U_0$ and the vortices velocity components $U_1$, $V_1$, and $W_1$.

### A. The mean flow

We consider the steady quasiparallel two-dimensional laminar flow past a surface with the streamwise cross section in the form of a circular arc with a large radius compared with the boundary-layer thickness. For this case, the mean flow can be approximated by the Blasius solution defined as

$$U_0\approx f(\eta), \qquad (34)$$

$$v_0\approx[1/2(x\,\mathrm{Re})^{1/2}][\eta f'(\eta)-f(\eta)], \qquad (35)$$

$$p_0\simeq\text{const}, \qquad (36)$$

where $\mathrm{Re}=U^*_\infty L^*/\nu^*$ is the Reynolds number based on the free-stream velocity $U^*_\infty$ and a characteristic length $L^*$,

$$\eta=y(\mathrm{Re}/x)^{1/2},$$

and $f$ is governed by the boundary-value problem

$$f'''+\tfrac{1}{2}ff''=0, \qquad (37a)$$

$$f=f'=0,\quad\text{at } \eta=0, \qquad (37b)$$

$$f'\to 1,\quad\text{as } \eta\to\infty. \qquad (37c)$$

### B. Goertler vortices

Although the present theory is applicable to any quasiperiodic counter-rotating streamwise vortices, we apply it to the case of Goertler vortices.

Following Floryan and Saric[7] and Ragab and Nayfeh,[8] we express the Goertler flow in normal-mode form as

$$\hat u=\rho_1(y)\exp\int\sigma\,dx_1\cos 2\beta z, \qquad (38a)$$

$$\hat v=R^{-1}\rho_3(y)\exp\int\sigma\,dx_1\cos 2\beta z, \qquad (38b)$$

$$\hat p=R^{-2}\rho_4(y)\exp\int\sigma\,dx_1\cos 2\beta z, \qquad (38c)$$

$$\hat w=R^{-1}\rho_5(y)\exp\int\sigma\,dx_1\cos 2\beta z, \qquad (38d)$$

where $\rho_1$, $\rho_3$, $\rho_4$, and $\rho_5$ are governed by the following eigenvalue problem:

$$\sigma\rho_1+D\rho_3+2\beta\rho_5=0, \qquad (39)$$

$$\left(D^2-4\beta^2-\sigma U_0-\frac{\partial U_0}{\partial x_1}\right)\rho_1-V_0\,D\rho_1-\rho_3\,DU_0=0, \qquad (40)$$

$$\begin{aligned}&(D^2-4\beta^2-\sigma U_0-DV_0)\rho_3-V_0\,D\rho_3\\&\quad-D\rho_4-\left(2\,\mathrm{GN}^2\,U_0+\frac{\partial V_0}{\partial x_1}\right)\rho_1=0,\end{aligned} \qquad (41)$$

$$(D^2-4\beta^2-\sigma U_0)\rho_5-V_0\,D\rho_5+2\beta\rho_4=0, \qquad (42)$$

$$\rho_1=\rho_3=\rho_5=0,\quad\text{at } y=0, \qquad (43)$$

$$\rho_n\to 0,\quad\text{as } y\to\infty. \qquad (44)$$

Floryan and Saric[7] and Ragab and Nayfeh[8] solved this eigenvalue problem using SUPORT.[9] Hall[10] questioned the normal-mode approach and solved the Goertler problem using a marching finite-difference scheme. His results indicate a large discrepancy between the two approaches. Day, Herbet, and Saric[11] and Kalburgi *et al.*[12] repeated the finite-difference calculations using reasonable initial conditions and found that the normal-mode approach is valid for vortices away from neutral conditions, and that the discrepancy noted by Hall is the result of using unreasonable initial conditions.

For certain $\beta$ and GN, we used the computer code developed by Ragab and Nayfeh[10] to calculate $\sigma_G=\sigma/R$ and the eigenfunctions $\rho_1$, $\rho_3$, $\rho_4$, and $\rho_5$ from Eqs. (39)–(44). Then we calculated $U_1=\rho_1$, $V_1=R^{-1}\rho_3$, $W_1=R^{-1}\rho_5$, and $P_1=R^{-2}\rho_4$, where $U_1$, $V_1$, $W_1$, and $P_1$ are the same as in Eqs. (28)–(31).

### C. Floquet problem

To solve the eigenvalue problem consisting of Eqs. (28)–(33) we rewrote these equations as a set of six first-order differential equations by defining

$$\xi_2 = D\xi_1 \quad \text{and} \quad \xi_6 = D\xi_5.$$

The result is

$$D\{\xi\} = [M(y)]\{\xi\} \pm \epsilon_v [C(y)]\{\xi\}, \tag{45a}$$

$$\xi_1 = \xi_3 = \xi_5 = 0, \quad \text{at } y=0, \tag{45b}$$

$$\xi_n \to 0, \quad \text{as } y \to \infty, \tag{45c}$$

where the vector $\{\xi\}$ is composed of $\xi_1$, $\xi_2$, $\xi_3$, $\xi_4$, $\xi_5$, and $\xi_6$, and the entries of the matrices $[M]$ and $[C]$ are defined in Appendix A. The resultant two point boundary-value problem consisting of Eqs. (45) is solved using the computer code SUPORT.[9]

## V. NUMERICAL RESULTS AND DISCUSSION

In all results, $\beta = 0.077\,463$ at the Reynolds number $R = 950$ based on $\delta_r = (\nu x^*/U_\infty)^{1/2}$, and GN = 12. Solving the Goertler problem as described earlier, we note that $V_1$, $W_1$, and $P_1$ are small compared with $U_1$. The growth rate $\sigma$ of the vortices was found to be 2.866 and hence $\sigma_G = \sigma/R = 0.003$. The corresponding eigenfunctions are shown in Fig. 1.

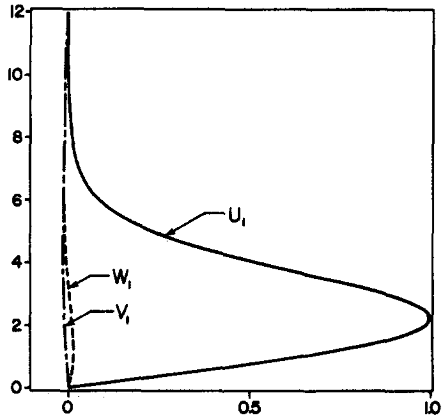


FIG. 1. Mode shapes of the Goertler vortex for GN = 12 and $2\beta = 0.154\,926$.

To compare the results of the present Floquet approach with those obtained using the method of multiple scales, we used Nayfeh's expression for the growth rate.[1] For the case of parallel flow, it reduces to

$$\gamma = -\alpha_i \pm \epsilon_v (\text{Real}) H_{12}, \quad H_{12} = h_{12}/g_{12}, \tag{46}$$

where $\gamma$ is the total growth rate of the excited TS wave, $-\alpha_i$ is the growth rate for the unperturbed TS wave, and $h_{12}$ and $g_{12}$ are coefficients defined in Appendix B in quadratures in terms of the eigenfunctions $\zeta_{mn}$ of the unperturbed TS wave problem and their adjoint eigenfunctions $\zeta^*_{mn}$. For a certain $\beta$, the three-dimensional code developed by Nayfeh and Padhye[13] was used to solve for $-\alpha_i$, $\zeta_{mn}$, and $\zeta^*_{mn}$. Then $h_{12}$ and $g_{12}$ were calculated using Appendix B and finally $\gamma$ was calculated from Eq. (46).

Using the streamwise velocity component $U_0$ of the Blasius flow and the vortex flow $U_1$, $V_1$, and $W_1$, and $\epsilon_v = 0.01$, we solved the eigenvalue problems consisting of Eqs. (28)–(33) obtained employing Floquet theory. The resulting growth rates for several frequencies are shown in columns 8 and 9 of Table I. The corresponding frequencies and unper-

TABLE I. Comparison of the total growth rates of TS waves predicted by the perturbation analysis with those obtained using Floquet theory; GN = 12, $\beta = 0.077\,463$, $R = 950$, $\sigma_G = 0.003$, and $\epsilon_v = 0.01$.

| | Unperturbed TS wave | | $H_{12}\times10^3$ | | $\gamma\times10^3$ predicted by perturbation solution | | $-\alpha_i\times10^3$ Floquet theory | |
|---|---|---|---|---|---|---|---|---|
| $F\times10^6$ | $\alpha_r$ | $-\alpha_i\times10^3$ | Real | Imag. | $\gamma^{(1)}$ | $\gamma^{(2)}$ | $-\alpha_i^{(1)}$ | $-\alpha_i^{(2)}$ |
| 80.0 | 0.2094 | −10.9184 | −46.843 | −43.893 | −10.450 | −11.386 | −10.438 | −11.410 |
| 75.0 | 0.1993 | −6.5857 | −38.543 | −24.000 | −6.201 | −6.972 | −6.195 | −6.965 |
| 72.5 | 0.1940 | −4.6718 | −35.532 | −9.005 | −4.316 | −5.027 | −4.316 | −5.026 |
| 70.0 | 0.1884 | −2.9346 | −28.376 | −10.806 | −2.651 | −3.219 | −2.649 | −3.216 |
| 67.5 | 0.1828 | −1.3750 | −24.922 | 0.139 | −1.126 | −1.624 | −1.126 | −1.624 |
| 65.0 | 0.1769 | 0.0089 | −18.395 | −2.500 | 0.174 | −0.193 | 0.174 | −0.194 |
| 62.5 | 0.1710 | 1.219 | 15.158 | 5.415 | 1.372 | 1.067 | 1.371 | 1.067 |
| 60.0 | 0.1650 | 2.2598 | −9.467 | 2.287 | 2.355 | 2.165 | 2.355 | 2.166 |
| 57.5 | 0.1589 | 3.1344 | 6.729 | −7.883 | 3.202 | 3.067 | 3.202 | 3.067 |
| 55.0 | 0.1527 | 3.8475 | −1.970 | 4.466 | 3.867 | 3.828 | 3.868 | 3.826 |
| 52.5 | 0.1464 | 4.4032 | −0.113 | −8.244 | 4.404 | 4.402 | 4.404 | 4.402 |
| 50.0 | 0.1401 | 4.8060 | 3.826 | 4.642 | 4.845 | 4.768 | 4.845 | 4.768 |
| 47.5 | 0.1337 | 5.061 | −5.160 | −6.964 | 5.113 | 5.009 | 5.112 | 5.009 |
| 45.0 | 0.1273 | 5.1712 | 7.672 | 3.227 | 5.248 | 5.095 | 5.241 | 5.095 |
| 42.5 | 0.1208 | 5.1430 | −8.145 | −4.371 | 5.224 | 5.062 | 5.224 | 5.061 |
| 40.0 | 0.1142 | 4.9810 | 9.217 | 6.537 | 5.073 | 4.889 | 5.073 | 4.889 |
| 37.5 | 0.1076 | 4.6903 | −8.663 | −0.753 | 4.777 | 4.604 | 4.777 | 4.603 |
| 35.0 | 0.1009 | 4.2774 | −7.942 | 3.106 | 4.357 | 4.198 | 4.355 | 4.198 |
| 32.5 | 0.0942 | 3.7490 | 6.121 | −3.525 | 3.810 | 3.688 | 3.810 | 3.687 |
| 30.0 | 0.0873 | 3.1130 | 3.120 | −7.213 | 3.145 | 3.081 | 3.145 | 3.082 |
| 27.5 | 0.0803 | 2.3808 | 0.261 | −7.825 | 2.383 | 2.378 | 2.384 | 2.379 |
| 25.0 | 0.0735 | 1.5640 | −6.078 | −6.109 | 1.625 | 1.503 | 1.626 | 1.505 |
| 21.0 | 0.0621 | 0.1272 | −16.878 | −12.349 | 0.042 | −0.292 | 0.040 | −0.298 |
| 20.0 | 0.0592 | −0.2472 | −20.000 | −12.354 | −0.047 | −0.447 | −0.046 | −0.445 |

TABLE II. Comparison of the total growth rates predicted using the perturbation analysis with those obtained using Floquet theory for several values of $\epsilon_v$, $F = 67.5\times10^{-6}$, $\beta = 0.077\,463$, $\sigma_G = 0.003$, GN = 12, $R = 950$, and $|\mathrm{Real}(H_{12})| = 24.922\times10^{-3}$.

| $\epsilon_v$ | Perturbation analysis $\times10^3$ | $\times10^3$ | Floquet theory $\times10^3$ | |
|---|---|---|---|---|
| 0.01 | $-1.126$ | $-1.624$ | $-1.126$ | $-1.624$ |
| 0.02 | $-0.877$ | $-1.873$ | $-0.878$ | $-1.873$ |
| 0.03 | $-0.627$ | $-2.123$ | $-0.632$ | $-2.119$ |
| 0.04 | $-0.329$ | $-2.372$ | $-0.389$ | $-2.362$ |
| 0.05 | $-0.129$ | $-2.621$ | $-0.148$ | $-2.600$ |
| 0.06 | 0.120 | $-2.870$ | 0.090 | $-2.827$ |
| 0.11 | 1.366 | $-4.116$ | 1.237 | $-3.737$ |

turbed eigenvalues are listed in columns 1, 2, and 3, respectively. Using the procedure described earlier, we calculated $H_{12}$ and $\gamma^{(1)}$ and $\gamma^{(2)}$ from Eq. (46). The results are listed in columns 4, 5, 6, and 7. Comparing columns 6 and 7 with columns 8 and 9 shows that the results of Floquet theory are in full agreement with those predicted by the perturbation analysis. Some of the values in columns 8 and 9 were obtained for both of the increased and decreased growth rates using only one form of Floquet solution.

Table II shows a comparison of the total growth rates predicted using the perturbation solution with those obtained using Floquet theory for several values of $\epsilon_v$. The agreement is fairly good even for $\epsilon_v = 0.11$. The good agreement may be because the eigenfunctions obtained using Floquet theory and shown in Fig. 2 are indistinguishable from the unperturbed TS waves, as shown in Fig. 2. In fact, the two sets of eigenfunctions cannot be distinguished for $\epsilon_v = 0.01$. This is in contrast with the case of subharmonic secondary instability for which the results predicted by the perturbation analysis do not agree with those obtained using Floquet theory.[14,15] In the subharmonic instability, the eigenfunctions obtained using Floquet theory are extremely different from the unperturbed TS eigenfunctions.

The frequency affects $\sigma_v$ by changing the positions of the peaks of the TS eigenfunctions compared with those of the Goertler vortices, the closer the two peaks are the more the contribution is. The contribution $\sigma_v = \epsilon_v|\mathrm{Real}(H_{12})|$ of the vortices to the growth rate of the TS waves, is shown in Fig. 3 as a function of the dimensionless frequency $F = \omega/R$. Figure 3 also shows that including the growth rate $\sigma_G$ of the vortices produces a slight change in their contribution to the growth rates of the TS waves.

Figure 4 shows the effect of $R$ on $\sigma_v$ for $\epsilon_v = 0.01$ and $F = 25\times10^{-6}$; $\sigma_v$ reaches zero at $R = 1060$ and $R = 2085$. Branch II of the unperturbed TS wave is at $R = 1660$. For $R > 1660$ there is no growing TS wave; instead there is a number of discrete eigenvalues, $\alpha$, that correspond to decaying TS waves, and hence there are different values of $\sigma_v$ depending on the value of $\alpha$ we choose. The $\sigma_v$ shown in Fig. 4 is the one corresponding to the continuation of the growing TS wave; $R$ was increased by a step of ten and the initial guess used for $\alpha$ is its value at the previous step. Similar to $F$, the Reynolds number $R$ influences $\sigma_v$ by changing the positions of the peaks of the TS eigenfunctions. The reason that

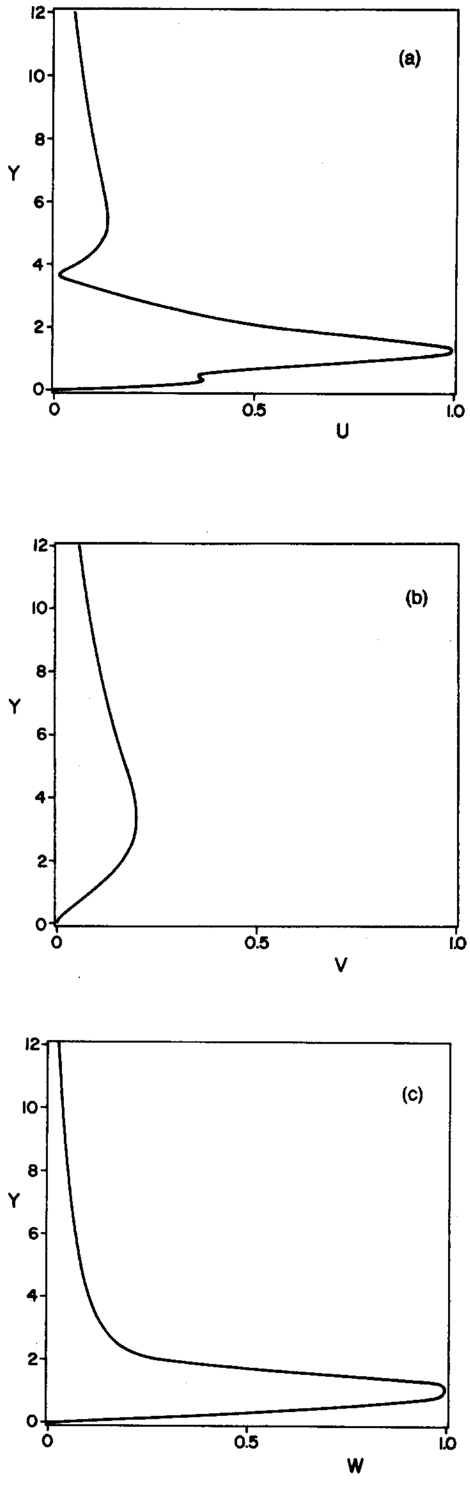


FIG. 2. The eigenfunctions of the perturbed TS wave obtained using Floquet theory: (a) streamwise component, (b) transverse component, and (c) spanwise component. Here $F = 27.5\times10^{-6}$, GN = 12, $R = 950$, and $\beta = 0.077\,463$.

the slope of $\sigma_v$ is discontinuous at $\sigma_v = 0$ in Figs. 3 and 4 is due to the fact that we plotted the absolute value of $\mathrm{Real}(H_{12})$. If we were to plot $\sigma_v$ and $-\sigma_v$ they will look like mirror images of each other.

It should be noted that the present analysis is valid only

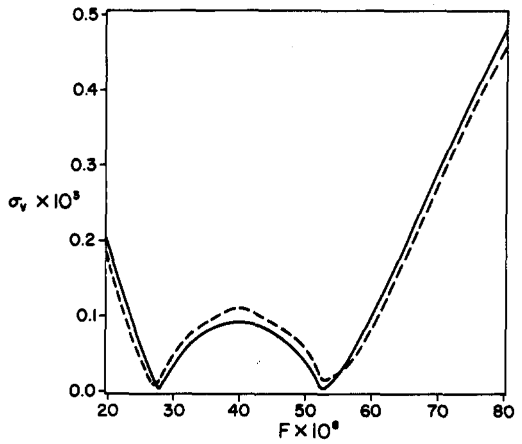


FIG. 3. Influence of the growth rate $\sigma_G$ of the vortices on their contribution to the growth rates of the TS waves: —, $\sigma_G$ is neglected; ---, $\sigma_G$ is included. Conditions are as in Table I.

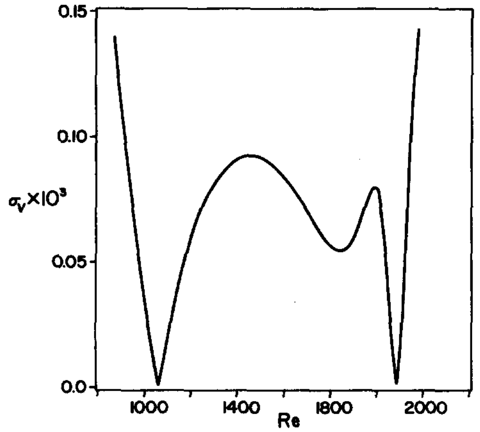


FIG. 4. Influence of the Reynolds number R on the contribution to the growth rates of the TS waves $\sigma_v$: $F = 25 \times 10^{-6}$, $\epsilon_v = 0.01$, GN = 12, at R = 950 and $\beta = 0.007\,463$.

when the amplitude $\epsilon_T$ of the oblique waves is small compared with the amplitude $\epsilon_v$ of the vortices. As the oblique waves grow, we need to account for the influence of these waves on the Goertler vortices. In fact, the oblique waves will generate streamwise vortices having an amplitude that is the order $\epsilon_T^2$, which may strengthen or weaken the primary vortices, depending on their phasings.

## ACKNOWLEDGMENT

This work was supported by the Office of Naval Research under Contract No. N00014-85-K-0011, NR 4325201.

## APPENDIX A: ENTRIES OF THE MATRICES [*M*] AND [*C*]

The matrix $[M]$ in Eq. (45a) is

$$[M] = \begin{bmatrix} 0 & 1 & 0 & 0 & 0 & 0 \\ \Lambda & 0 & R\,DU & i\alpha R_0 & 0 & 0 \\ -i\alpha & 0 & 0 & 0 & -i\beta & 0 \\ 0 & -i\alpha/R & -\Lambda/R & 0 & 0 & -i\beta/R \\ 0 & 0 & 0 & 0 & 0 & 1 \\ 0 & 0 & 0 & i\beta R & \Lambda & 0 \end{bmatrix},$$

where

$$\Lambda = iR(\alpha U_0 - \omega) + \alpha^2 + \beta^2.$$

The matrix $[C]$ in Eq. (45a) is

$$[C] = \frac{1}{2}\begin{bmatrix} 0 & 0 & 0 & 0 & 0 & 0 \\ R(i\alpha U_1 - \beta W_1) & RV_1 & R\,DU_1 & 0 & -iR\beta U_1 & 0 \\ 0 & 0 & 0 & 0 & 0 & 0 \\ i\alpha V_1 & 0 & -(i\alpha U_1 - \beta W_1 + V_1) & 0 & i3\beta V_1 & 0 \\ 0 & 0 & 0 & 0 & 0 & 0 \\ 0 & 0 & -iR\,DW_1 & 0 & -R(i\alpha U_1 + \beta W_1) & -RV_1 \end{bmatrix}.$$

## APPENDIX B: DEFINITIONS OF $h_{12}$ AND $g_{12}$

The coefficients of modulation equations are

$$g_{11} = g_{21} = \int_0^\infty (\zeta_{11}\zeta_{11}^* + \zeta_{31}\zeta_{31}^* + \zeta_{51}\zeta_{51}^*)dy, \tag{B1}$$

$$\begin{aligned} h_{12} = h_{21} = \frac{1}{2}\int_0^\infty \bigg[ & \zeta_{11}^*\left((i\alpha + \sigma_G)U_1\zeta_{12} + V_1\frac{\partial \zeta_{12}}{\partial y} + \frac{\partial U_1}{\partial y}\zeta_{32} - \beta W_1\zeta_{12} - 2i\beta U_1\zeta_{52}\right) \\ & + \zeta_{31}^*\left(i\alpha U_1\zeta_{32} + \frac{\partial}{\partial y}(V_1\zeta_{32}) + \sigma_G V_1\zeta_{32} - \beta W_1\zeta_{32} - 2i\beta V_1\zeta_{52}\right) + \zeta_{51}^*\bigg(i\alpha U_1\zeta_{52} + \beta W_1\zeta_{52} \\ & + V_1\frac{\partial \zeta_{52}}{\partial y} + i\sigma_G W_1\zeta_{12} + i\frac{\partial W_1}{\partial y}\zeta_{32}\bigg)\bigg]dy. \end{aligned} \tag{B2}$$

The eigenvalue problem for the unperturbed TS wave is

$$i\alpha\zeta_{1n} + D\zeta_{3n} + (-1)^n i\beta\zeta_{5n} = 0, \tag{B3}$$

$$i(\alpha U_0 - \omega)\zeta_{1n} + \zeta_{3n}\, DU_0 + i\alpha\zeta_{4n} - (1/R)(D^2 - \alpha^2 - \beta^2)\zeta_{1n} = 0, \tag{B4}$$

$$i(\alpha U_0 - \omega)\zeta_{3n} + D\zeta_{4n} - (1/R)(D^2 - \alpha^2 - \beta^2)\zeta_{3n} = 0, \tag{B5}$$

$$i(\alpha U_0 - \omega)\zeta_{5n} + (-1)^n i\beta\zeta_{4n} - (1/R)(D^2 - \alpha^2 - \beta^2)\zeta_{5n} = 0, \tag{B6}$$

$$\zeta_{1n} = \zeta_{3n} = \zeta_{5n} = 0, \quad \text{at } y = 0, \tag{B7}$$

$$\zeta_{mn} \to 0, \quad \text{as } y \to \infty, \tag{B8}$$

where $D = \partial/\partial y$.

The adjoint problem can be represented by

$$i\alpha\zeta^*_{1n} - D\zeta^*_{3n} + (-1)^n i\beta\zeta^*_{5n} = 0, \tag{B9}$$

$$i(\alpha U_0 - \omega)\zeta^*_{1n} + i\alpha\zeta^*_{4n} - (1/R)(D^2 - \alpha^2 - \beta^2)\zeta^*_{1n} = 0, \tag{B10}$$

$$i(\alpha U_0 - \omega)\zeta^*_{3n} - D\zeta^*_{4n} + \zeta^*_{1n}\, DU_0 - (1/R)(D^2 - \alpha^2 - \beta^2)\zeta^*_{3n} = 0, \tag{B11}$$

$$i(\alpha U_0 - \omega)\zeta^*_{5n} + (-1)^n i\beta\zeta^*_{4n} - (1/R)(D^2 - \alpha^2 - \beta^2)\zeta^*_{5n} = 0, \tag{B12}$$

$$\zeta^*_{1n} = \zeta^*_{3n} = \zeta^*_{5n} = 0, \quad \text{at } y = 0, \tag{B13}$$

$$\zeta^*_{mn} \to 0, \quad \text{as } y \to \infty. \tag{B14}$$


[1]A. H. Nayfeh, J. Fluid Mech. **107**, 441 (1981).
[2]Th. Herbert and M. V. Morkovin, in *Laminar-Turbulent Transition*, edited by R. Eppler and H. Fasel, IUTAM Symposium, Stuttgart, Germany (Springer, New York, 1979), p. 37.
[3]J. M. Floryan and W. S. Saric, AIAA Paper No. 80-1376, 1980.
[4]M. R. Malik, AIAA Paper No. 86-1129, 1986.
[5]K. M. Srivastava and U. Dallmann, Phys. Fluids **30**, 1005 (1987).
[6]J. Bennett and P. Hall, NASA Report No. 178221, 1986.
[7]J. M. Floryan and W. S. Saric, AIAA J. **20**, 316 (1982).
[8]S. A. Ragab and A. H. Nayfeh, Phys. Fluids **24**, 1405 (1981).
[9]R. R. Scott and H. A. Watts, SIAM J. Numer. Anal. **14**, 40 (1977).
[10]P. Hall, J. Fluid Mech. **130**, 41 (1983).
[11]H. P. Day, Th. Herbert, and W. S. Saric (private communication).
[12]V. Kalburgi, S. M. Mangalam, J. R. Dagenhart, and S. N. Tiwari, *Research in National Laminar Flow and Laminar-Flow Control* (NASA, Washington, DC, 1987), p. 289.
[13]A. H. Nayfeh and A. Padhye, AAIA J. **17**, 1084 (1979).
[14]Th. Herbert, AIAA Paper No. 84-0009, 1984.
[15]A. H. Nayfeh, AIAA Paper No. 85-1697, 1985.